
10-1-2004

Simultaneous Measurement of Middle-Ear Input Impedance and Forward/Reverse Transmission in Cat

Susan E. Voss

Smith College, svoss@smith.edu

Christopher A. Shera

Massachusetts Eye and Ear Infirmary

Follow this and additional works at: https://scholarworks.smith.edu/egr_facpubs



Part of the [Engineering Commons](#)

Recommended Citation

Voss, Susan E. and Shera, Christopher A., "Simultaneous Measurement of Middle-Ear Input Impedance and Forward/Reverse Transmission in Cat" (2004). Engineering: Faculty Publications, Smith College, Northampton, MA.

https://scholarworks.smith.edu/egr_facpubs/75

This Article has been accepted for inclusion in Engineering: Faculty Publications by an authorized administrator of Smith ScholarWorks. For more information, please contact scholarworks@smith.edu

Simultaneous measurement of middle-ear input impedance and forward/reverse transmission in cat

Susan E. Voss^{a)}

*Picker Engineering Program, Smith College, 51 College Lane, Northampton, Massachusetts 01063
and Eaton-Peabody Laboratory of Auditory Physiology, Massachusetts Eye and Ear Infirmary,
243 Charles Street, Boston, Massachusetts 02114*

Christopher A. Shera

*Eaton-Peabody Laboratory of Auditory Physiology, Massachusetts Eye and Ear Infirmary, 243 Charles
Street Boston, Massachusetts 02114 and Department of Otolaryngology, Harvard Medical School,
Boston, Massachusetts 02115*

(Received 29 January 2004; revised 2 July 2004; accepted 6 July 2004)

Reported here is a technique for measuring forward and reverse middle-ear transmission that exploits distortion-product otoacoustic emissions (DPOAEs) to drive the middle ear “in reverse” without opening the inner ear. The technique allows measurement of DPOAEs, middle-ear input impedance, and forward and reverse middle-ear transfer functions in the same animal. Intermodulation distortion in the cochlea generates a DPOAE at frequency $2f_1 - f_2$ measurable in both ear-canal pressure and the velocity of the stapes. The forward transfer function is computed from stapes velocities and corresponding ear-canal pressures measured at the two primary frequencies; the reverse transfer function is computed from velocity and pressure measurements at the DPOAE frequency. Middle-ear input impedance is computed from ear-canal pressure measurements and the measured Thévenin equivalent of the sound-delivery system. The technique was applied to measure middle-ear characteristics in anesthetized cats with widely opened middle-ear cavities (0.2–10 kHz). Stapes velocity was measured at the incudo-stapedial joint. Results on five animals are reported and compared with a published middle-ear model. The measured forward transfer functions and input impedances generally agree with previous measurements, and all measurements agree qualitatively with model predictions. The reverse transfer function is shown to depend on the acoustic load in the ear canal, and the measurements are used to compute the round-trip middle-ear gain and delay. Finally, the measurements are used to estimate the parameters of a two-port transfer-matrix description of the cat middle ear. © 2004 Acoustical Society of America. [DOI: 10.1121/1.1785832]

PACS numbers: 43.64.Bt, 43.64.Jb, 43.64.Ha [WPS]

Pages: 2187–2198

I. INTRODUCTION

The middle ear’s primary function of coupling acoustic signals from the ear canal to the cochlea has been well recognized for over 100 years (reviewed in Merchant and Rosowski, 2003). With the discovery of otoacoustic emissions (OAEs) the recognized role of the middle ear expanded: not only does the middle ear couple external sounds to the cochlea, but it also couples sounds generated within the cochlea back to the ear canal. Describing the transmission characteristics of the middle ear in both the forward and the reverse directions is critical for many purposes, including understanding the middle-ear’s effects on OAEs and understanding middle-ear function in both normal and diseased ears in order to develop better therapeutic and diagnostic approaches for pathological middle ears.

Recent work has focused on middle-ear transmission in both the forward and the reverse directions (e.g., Puria and Rosowski, 1996; Magnan *et al.*, 1997, 1999; Avan *et al.*, 2000; Puria, 2003, 2004). However, quantitative descriptions (measurement or model) of both forward- and reverse-

transfer functions of the middle ear are not sufficient to completely describe the middle ear’s function, as these transfer functions depend on terminating impedances (i.e., cochlear impedance and ear-canal impedance directed outward from the ear canal). Instead of describing the middle ear’s function through specific transfer functions, the middle ear can be regarded as a black box whose input–output relations can be described without reference to its specific components or to its termination (Shera and Zweig, 1991, 1992b; Puria, 2003, 2004). Mathematically, these input–output relations can be described using a two-port model characterized by a 2×2 transfer matrix [sometimes called an “*ABCD* matrix” after its four matrix elements, which are traditionally denoted $\begin{pmatrix} A & B \\ C & D \end{pmatrix}$]. If the load impedances are known, measurement of four independent, complex functions of frequency completely determines the values of the four matrix elements. In practice, at least one of these four measurements must be obtained while driving the middle ear “in reverse” (i.e., from within the inner ear).

Despite its considerable importance both for testing models of middle-ear mechanics and for understanding the effects of middle-ear transmission on OAEs, a complete two-port characterization of the input–output relations of the

^{a)}Electronic mail: svoss@email.smith.edu

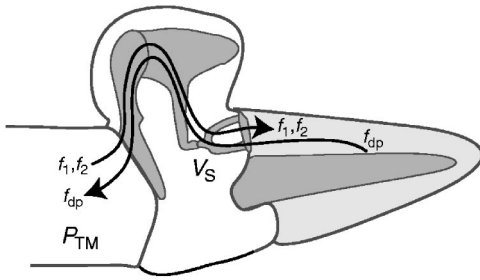


FIG. 1. Schematic diagram illustrating the idea behind the method. Primary stimulus tones (at frequencies f_1 and f_2) drive the middle ear in the forward direction while the distortion-product (at frequency f_{dp}) drives the middle ear “in reverse.” Forward and reverse middle-ear transfer functions can be computed from measurements of ear-canal pressure (P_{TM}) and stapes velocity (V_S).

middle ear has so far only been obtained in human temporal bones (Puria, 2003). Much of the technical difficulty in obtaining this characterization comes from the need to measure the cochlear response (e.g., stapes velocity or intracochlear pressure) while driving the middle ear in reverse (e.g., with a hydrophone in the vestibule). For example, inserting transducers into the inner ear can introduce tiny air bubbles into the scalae that, unless carefully controlled for, significantly alter the measured responses (Puria *et al.*, 1997). As a step towards obtaining a two-port characterization of a living middle ear, we have developed a method for measuring forward and reverse middle-ear transmission that exploits distortion-product otoacoustic emissions (DPOAEs) to drive the middle ear in reverse without opening the inner ear. The technique allows for the measurement of DPOAEs, middle-ear input impedance, and forward and reverse middle-ear stapes-velocity transfer functions in the same animal. The ability to measure all of these quantities in the same preparation allows for experimentally based estimates of the transfer matrix that are not compromised by interanimal variations in the measurements. A preliminary account of this work has been presented elsewhere (Voss and Shera, 2002).

II. METHODS

A. Overview of the method

The idea behind the measurement is illustrated in Fig. 1. When the cochlea is stimulated by primary tones at frequencies f_1 and f_2 (with $f_2 > f_1$), intermodulation distortion in the cochlea generates energy at the combination-tone frequency $f_{dp} = 2f_1 - f_2$ that propagates back along the cochlear partition. When it reaches the base of the cochlea, some of this energy vibrates the stapes and is subsequently transmitted through the middle ear to the ear canal, where it can be measured as a DPOAE. Energy at the three frequencies f_1 , f_2 , and f_{dp} is therefore measurable in both the stapes velocity and the ear-canal pressure; in effect, the primary tones drive the middle ear in the forward direction while the distortion-product drives the middle ear “in reverse.” Simultaneous measurements of forward transmission (at f_1 and f_2) and reverse transmission (at f_{dp}) can therefore be performed by extracting the appropriate frequency components from the measured ear-canal pressure and stapes velocity using Fourier analysis. Note that for the method to yield reliable mea-

surements of reverse transmission it is crucial that the dominant sources of energy at f_{dp} measured in the ear canal lie on the cochlear side of the middle ear (i.e., within the cochlea or annular ligament).

B. Definitions of transfer functions

The forward stapes-velocity transfer function, $\vec{T}_S(f)$, is a measure of the transmission from the ear canal through the middle ear to the stapes. \vec{T}_S is defined as the ratio of stapes velocity (V_S) to the ear-canal pressure at the tympanic membrane (P_{TM}) when the middle ear is driven from the ear canal (i.e., at frequencies f_1 and f_2):

$$\vec{T}_S(f) \equiv \frac{V_S(f)}{P_{TM}(f)}, \quad f \in \{f_1, f_2\}. \quad (1)$$

When the middle ear is driven in the forward direction, we adopt the convention that a positive displacement moves the stapes into the cochlea.

The reverse stapes-velocity transfer function, $\overleftarrow{T}_S(f)$, measures the transmission from the stapes back through the middle ear to the ear canal. \overleftarrow{T}_S is defined as the ratio of P_{TM} to V_S when the middle ear is driven from within the cochlea (i.e., at the frequency f_{dp}):

$$\overleftarrow{T}_S(f_{dp}) \equiv \frac{P_{TM}(f_{dp})}{V_S(f_{dp})}. \quad (2)$$

In this case, a positive displacement moves the stapes out of the cochlea. The left- and rightward pointing arrows atop the transfer functions \vec{T}_S and \overleftarrow{T}_S indicate both the forward and reverse directions and the assumed polarity of positive displacements.

C. Animal preparation

Measurements were made on one ear in each of five anesthetized cats. Treatment of animal subjects accorded with protocols approved by the animal care committee at the Massachusetts Eye and Ear Infirmary.

Young cats weighing between 2.15 and 2.50 kg were anesthetized with intraperitoneal injections of Dial (75 mg/kg). Booster doses of Dial (10% of the initial dose) were given throughout the experiments, as indicated by either a withdrawal response to a toe pinch or an increase of 20% in heart rate. Cats were also connected to a saline drip in order to keep them hydrated for the duration of the experiment. All measurements were performed in a humidified sound-proof booth maintained at approximately 38 °C.

The pinna and most of the cartilaginous ear canal were removed to allow the sound source to be placed close to the tympanic membrane. The ventral and lateral walls of the bulla and most of the bony septum were removed so that the middle ear was opened widely. As illustrated in Fig. 2, access to the stapes was obtained by drilling the bone lateral to the superior-posterior quadrant of the tympanic membrane (Tonndorf and Tabor, 1962). As described by Tonndorf and Tabor (1962):

“[The hole’s] location corresponds to McEwen’s triangle in man: posterior to the rim of the eardrum, in-

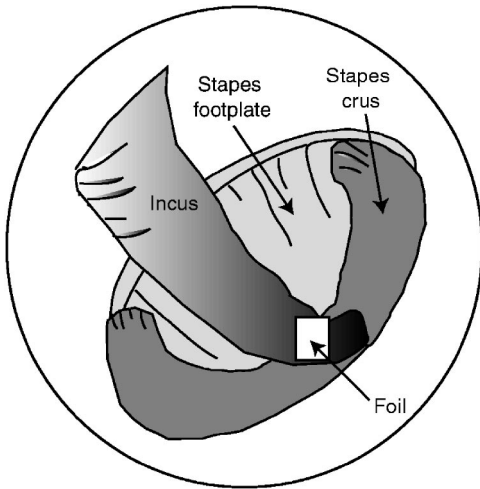


FIG. 2. Schematic of the view of the stapes after drilling the location in cat that corresponds to McEwen's triangle in man (adapted from Fig. 4 of Tonndorf and Tabor, 1962). The white rectangle labeled "Foil" indicates the location of the reflective tape used during velocity measurements to reflect the laser beam.

ferior to the inferior temporal line and anterior-superior to the mastoid ridge. This perforation opens directly over the incudo-stapedial joint, giving good access to the anterior two-thirds of the footplate and to the anterior crus. ... (Care must be taken not to cut into the underlying soft tissues as bleeding from the mastoid vessels is very annoying.)"

To determine the effects of drilling on cochlear sensitivity we measured ear-canal DPOAEs both before and after drilling McEwen's triangle in three of the five ears. Since differences between pre- and postdrilling emissions differed by less than 5 dB at most frequencies, we conclude that the drilling had little effect on the emissions generated by the cochlea. While changes in emissions before and after drilling have no effect on our measured transfer functions, it was important to determine that after drilling the cochlea was still generating a substantial and robust distortion product.

D. Stimulus generation and response measurement

Ear-canal pressures (P_{EC}) were generated and measured with calibrated transducers positioned within 2–3 mm of the tympanic membrane and controlled by a computer running LabVIEW (detailed in Shera and Guinan, 1999). The earphones were two $\frac{1}{4}$ -in. Larson-Davis microphones used as sound sources; the microphone was an Etymotic ER-10C. The stimulus was either a broadband chirp (used to measure impedance) or two pure tones at primary frequencies f_1 and f_2 (used to measure forward and reverse transfer functions). To reduce the possibility of distortion in the earphone system, each of the two primary tones was produced by its own earphone. The primary-tone frequency ratio f_2/f_1 and level difference $L_1 - L_2$ were chosen with the goal of maximizing the magnitude of the resulting distortion product (f_2/f_1 was fixed at the value 1.2 and $L_1 - L_2$ was typically 5 to 10 dB). Response magnitudes and angles were obtained from the 4096-point discrete Fourier transform of the time-domain average of N responses ($64 \leq N \leq 1024$) sampled at 44.04 kHz.

E. Measurement of stapes velocity

After exposing the stapes via McEwen's triangle, we placed a small reflective foil on the long process of the incus, at the incudo-stapedial joint (see Fig. 2). The velocity of this foil was measured with a laser vibrometer (Polytec OFV-501). Guinan and Peake (1967) have shown that no significant slippage occurs between the incus and the stapes at the incudo-stapedial joint (i.e., the joint is effectively rigid in cat); this assumption is consistent with the more recent work of Decraemer and colleagues (Decraemer, 2004a,b). We therefore refer to the measured velocity as the stapes velocity, V_S . The Doppler-shifted reflected signal was detected and decoded by the vibrometer to produce an output voltage proportional to stapes velocity (detailed in Voss *et al.*, 2000). The vibrometer output voltage was amplified by a factor of 10.

The laser vibrometer system measures velocity in the direction of the laser beam. Here, the laser beam was focused on the incudo-stapedial joint, and the angle between the laser beam and the pistonlike stapes motion was judged visually to be close to zero. Any small nonzero angle would have negligible effects on the results reported here. For example, if the angle had been 20° , the measurements reported here would systematically underestimate the true velocity by only 0.5 dB (i.e., $20 \log_{10}[\cos(20\pi/180)]$).

We assume that the mass of the foil (0.05 mg) had a negligible effect on the motion of the ossicular system since the mass of the foil was substantially smaller than the mass of the stapes (0.530 ± 0.05 mg) and the incus (4.313 ± 0.328 mg) (Lynch, 1981). Additional support for this assumption comes from control measurements reported by Voss (1998, Figs. 1–4) where stapes velocity measurements are shown to be similar when measured using either a single foil (mass 0.05 mg) or with three foils (0.15 mg). Thus, these measurements are consistent with the assumption that the foil has little effect on the mechanics of the middle-ear system.

F. Noise floor for stapes-velocity measurements

We obtained estimates of the noise floor for the velocity measurements by (1) measuring the velocity of the skull in response to the ear-canal stimulus and/or (2) measuring the stapes velocity in the absence of the stimulus. Both methods produced similar estimates of the noise floor. One measured noise floor for the stapes-velocity magnitude is plotted as circles in the top-center plot of Fig. 4. Here, and in all experiments, the measured noise floor has been filtered with a median filter in order to smooth the noise floor across the measured frequency range. The effect of the median filter on the noise floor is illustrated by the line labeled "filtered noise floor." The magnitude of the stapes velocity at the distortion-product frequency ($|V_S(f_{dp})|$) was substantially smaller than that at the primary frequencies ($|V_S(f_1)|$ and $|V_S(f_2)|$) and was often corrupted by noise. In our plots of the reverse transfer function (Fig. 5), we do not plot data points for which the noise floor was within 10 dB of the measured stapes velocity. The noise floor limited the measurement of

the reverse transfer function at the lower frequencies. Measurements of the forward transfer function were always more than 10 dB above the noise floor.

G. Source of intermodulation distortion

The method described here assumes that the dominant sources of intermodulation distortion originate on the cochlear side of the middle ear (i.e., within the cochlea and/or the annular ligament). Although it is well documented that the cochlea produces intermodulation distortion, there is little experimental evidence about the magnitude of middle-ear intermodulation distortion, although the documented linearity of middle-ear mechanics at the driving frequency suggests that it is small. Here we assume that middle-ear intermodulation distortion at $2f_1 - f_2$ is small compared to that generated within the cochlea or annular ligament.

Postmortem measurements made in one of our preparations support this assumption for frequencies above 2 kHz. Specifically, at ear-canal sound pressure levels of 85 and 80 dB SPL for f_1 and f_2 , respectively, ear-canal distortion products measured 2 h postmortem decreased by 15 to 30 dB between 0.7 and 7 kHz. The stapes velocity at f_{dp} decreased by the same factor for frequencies above 2 kHz; for many measurements above 2 kHz the decrease was equivalent to a reduction to the level of the noise floor. For measurements between 0.7 and 2 kHz, the results are not so clear cut. Stapes velocity at f_{dp} did not always decrease proportionally with the ear-canal pressure at f_{dp} . About half of these data points were within the noise floor. Further study is clearly needed to quantify the magnitude and sources of any intermodulation distortion originating within the middle ear.

H. Impedance measurements

The middle-ear input impedance, $Z_{EC}(f)$, was calculated from the ear-canal pressure (P_{EC}) and the Thévenin equivalent impedance (Z_{Th}) and pressure (P_{Th}) of the transducer (e.g., Allen, 1986; Keefe *et al.*, 1992; Voss and Allen, 1994; Neely and Gorga, 1998). Pressure measurements made in six cylindrical tubes provided six complex equations for the two unknown Thévenin equivalents, Z_{Th} and P_{Th} . Acoustic estimates of the tube lengths were obtained by minimizing the error function in the overdetermined system of six equations (Allen, 1986; Keefe *et al.*, 1992), and the optimized lengths were used to compute Z_{Th} and P_{Th} . Results were checked by comparing measured and theoretical impedances in five additional tubes. At frequencies in the range 0.2–10 kHz the measured impedances were within 1 dB in magnitude and 0.01 cycles in angle of the corresponding theoretical impedances, except at maxima and minima in the impedance, where the estimates depend heavily on the precise length of the tube; at these frequencies the differences approached 5 dB in magnitude and 0.05 cycles in angle.¹

I. Effect of higher-order modes

Our description of the measurements (i.e., impedance and forward and reverse transmission) assumes plane-wave propagation and that any higher-order spatial modes are neg-

ligible. Two theoretical sources for higher-order modes exist: (1) complex wave motion on the tympanic membrane that produces evanescent pressure modes in the ear canal near the tympanic membrane and (2) evanescent modes near the probe microphone that result from the stimulus pressure generation. Using both theoretical and measurement-based explanations, Lynch (1981) (pp. 146–148) argues that evanescent pressure modes generated by the tympanic membrane are insignificant for a probe tube placed within a few mm of the tympanic membrane at frequencies up to 22.4 kHz. Although evanescent modes produced by the earphone presumably contribute to the total pressure recorded by the microphone, our ability to accurately measure the impedance of test cavities using the Thévenin equivalents of our sound source suggests that the total contribution of these modes is small at frequencies below 10 kHz. Although our transducer assembly had a short probe-tube extension (<1 mm), the work of Huang *et al.* (2000a,b) suggests that a longer “probe-tube extension” is needed above about 2 kHz to eliminate evanescent-wave contributions from the pressure source. However, an important difference between our work and the work of Huang *et al.* (2000a,b) is that we work in domestic cat near the tympanic membrane where the cross-sectional dimensions of the ear canal are significantly smaller than the range of dimensions explored by Huang *et al.* (2000a,b).

J. Accounting for the residual ear-canal air space

The probe microphone that measured the ear-canal sound pressure was positioned about 3 mm from the tympanic membrane. We model the residual ear-canal air space between the probe microphone and the tympanic membrane as a rigid-walled cylindrical tube with uniform, plane-wave propagation occurring for frequencies below 10 kHz. In this case, the pressure and volume velocity at the probe microphone (P_{EC}, U_{EC}) are related to their counterparts at the tympanic membrane (P_{TM}, U_{TM}) by the transfer matrix

$$\begin{pmatrix} P_{EC} \\ U_{EC} \end{pmatrix} = \begin{pmatrix} \cosh(ikl) & Z_0 \sinh(ikl) \\ 1/Z_0 \sinh(ikl) & \cosh(ikl) \end{pmatrix} \begin{pmatrix} P_{TM} \\ U_{TM} \end{pmatrix}, \quad (3)$$

where $Z_0 = \rho c/A$ is the characteristic impedance of the tube, l is the length of the cylindrical air-filled tube, A is the cross-sectional area of the tube, $k = 2\pi f/c$ is the wavenumber, ρ is the density of air, c is the velocity of sound in air, and f is the frequency (e.g., Møller, 1965; Rabinowitz, 1981; Lynch *et al.*, 1994; Huang *et al.*, 1997; Voss *et al.*, 2000). We assume that the effective area of the equivalent coupling tube is equal to the area of the source tube (radius $a = 2.8$ mm). Although we did not measure the exact volume or dimensions of the air space in our cats, the equivalent volume was measured by Lynch *et al.* (1994) in six animals prepared in a similar manner to ours. Their volumetric measurements ranged from 62 to 75 mm³; we approximate the volume in our preparations by their mean value of 68.5 mm³ and the distance l from the probe microphone to the tympanic membrane by $l = 68.5/\pi a^2 = 2.74$ mm, a value consistent with our estimate of 3 mm.

In the forward direction, application of Eq. (3) is consistent with the findings of Lynch *et al.* (1994), who found

only small differences between Z_{EC} and Z_{TM} at frequencies below about 6 kHz but larger differences at higher frequencies, where the impedance ratio was approximately 3 dB in magnitude and up to 0.20 cycles in angle. In contrast, application of Eq. (3) results in ratios P_{TM}/P_{EC} that are nearly 1 at all frequencies up to 10 kHz; across all ears and in narrow bands the magnitude of the pressure ratio ranges from 0.85 to 1.20, but at most frequencies it is within 0.95 to 1.02 (i.e., a variation of less than 0.5 dB). The angle difference is generally within 0.02 cycles of zero.

In the reverse direction, the ear-canal air space also influences our measurements and model. In this case, the load on the ear-canal air space is the Thévenin impedance of the source, Z_{Th} . Thus, the total load at the tympanic membrane in the reverse direction is the ear-canal air space terminated by Z_{Th} . We define this load as $Z_{SRC} = P_{TM}/U_{TM}$. Consistent with the findings in the forward direction, in the reverse direction Z_{Th} and Z_{SRC} differ by substantial amounts while P_{EC} and P_{TM} are similar. In the reverse direction, the ratio Z_{SRC}/Z_{Th} has a magnitude near one and an angle near zero for frequencies below 1 kHz, but the magnitude varies by a factor of 1.5–3 at most frequencies between 1 and 10 kHz with corresponding angle variations between 0.1 and 0.25 cycles. The ratio P_{TM}/P_{EC} in the reverse direction is between 0.9 and 1.1 in magnitude and within 0.025 cycles of zero in angle.

All data presented here use P_{TM} and Z_{TM} obtained from measurements of P_{EC} and Z_{EC} using Eq. (3).

K. Stability of the preparation

We observed substantial variation in the stability of our preparations. In all cases, preparations were sensitive to drying-out effects (e.g., Voss *et al.*, 2000); although we humidified the warm chamber air, exposing the middle-ear system apparently caused the ossicular system to dry out and stiffen over time. This effect was manifest as an increase in the ear's impedance and a decrease in the low-frequency magnitude of the stapes velocity. In some, but not all cases, these effects were reversed by moistening the middle ear with saline. In several of the experiments, middle-ear bleeding ultimately led to problems with the stability of the preparation; in some of these cases the bleeding was controlled for several hours through periodic gentle suction and bone wax, but a large blood clot would ultimately form over the stapes, making further measurements impossible. Further confounding the problem was the fact that a single measurement session that swept a wide frequency range typically took several hours, since a large number of averages were needed to reduce the noise floor. Changes in middle-ear impedance were readily observable when the computer-controlled voltage to the earphone no longer produced the expected sound pressure levels. (The expected sound pressure was based upon an in-the-ear calibration performed periodically during the experiments; changes in ear-canal impedance resulted in changes in this calibration and thus in the ear-canal pressure produced.) We used deviations in the ear-canal sound levels L_1 and L_2 from their expected values as an indication that the impedance of the system had changed. In all measure-

ments reported here, L_1 and L_2 are within 1.5 dB of their expected values. When changes in either the impedance magnitude or the low-frequency stapes-velocity magnitude occurred, measurements were aborted and attempts to return the system to its original response were made via moistening the middle ear and tympanic membrane with saline. If these attempts failed, measurements were ceased. Although the measurements shown in Fig. 4 at several stimulus levels were made over a 4-h period when the preparation was stable, the results presented here are generally the measurements made at the beginning of the measurement session on each ear.

III. RESULTS

We measured DPOAEs, middle-ear input impedance, and forward and reverse stapes-velocity transfer functions in each of five ears. Figure 3 illustrates the calculation of forward and reverse transfer functions. The transfer functions $\overrightarrow{T}_S(f)$ and $\overleftarrow{T}_S(f)$ (right panel) were computed from ear-drum pressures P_{TM} (left panel) and stapes velocities V_S (center panel) measured simultaneously in response to primary tones at frequencies f_1 and f_2 . Results are plotted for frequencies in the range 0.2–10 kHz. Measurements of the forward and reverse transmission are plotted for all frequencies that they were measured at within the 0.2–10 kHz range; in some cases the measurements only cover part of the frequency range.

A. Linearity of forward and reverse transmission

Consistent with previous findings (e.g., Wever and Lawrence, 1954; Guinan and Peake, 1967; Buunen and Vlaming, 1981; Voss *et al.*, 1996), forward middle-ear transmission appears to be linear. In our results, stapes velocities at f_1 and f_2 grow linearly with ear-canal sound pressure over the range of stimulus levels used (40–100 dB SPL). Figure 4 shows that reverse transmission also appears linear. The left-hand column plots the ear-canal DPOAEs $P_{TM}(f_{dp})$ measured at several different primary levels. The middle column plots the corresponding distortion-product components of the stapes velocity, $V_S(f_{dp})$. The right-hand column plots the reverse middle-ear transfer function $\overleftarrow{T}_S(f_{dp})$, defined as the ratio P_{TM}/V_S . Although both $P_{TM}(f_{dp})$ and $V_S(f_{dp})$ depend nonlinearly on the primary stimulus levels (L_1 and L_2), the reverse transfer function $\overleftarrow{T}_S(f)$ appears approximately independent of V_S , consistent with linear behavior. Note, however, that in the reverse direction the range of stapes velocities explored (15 dB) is considerably smaller than in the forward direction (60 dB). The range we were able to explore is bounded from below by the measurement noise floor and from above by the magnitude of the distortion generated within the cochlea.

B. Forward and reverse transfer functions

Figure 5 shows our measurements of $\overrightarrow{T}_S(f)$ and $\overleftarrow{T}_S(f)$ on five ears. The figure also compares our results with the measurements of Guinan and Peake (1967) and with the predictions of the middle-ear model of Puria and Allen (1998).

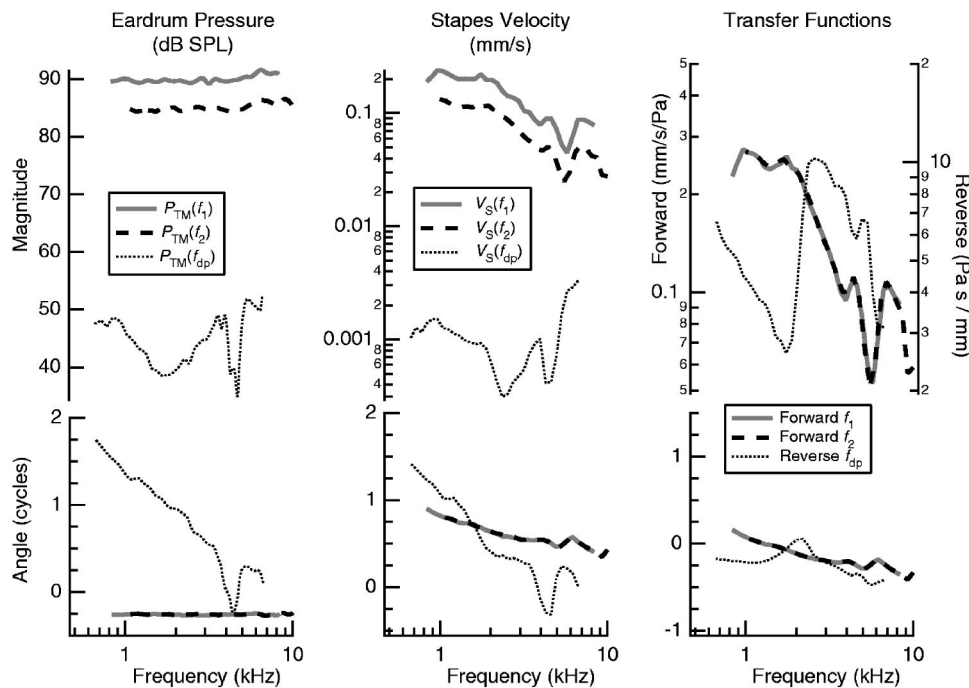


FIG. 3. Magnitudes (upper) and angles (lower) of simultaneous measurements of eardrum pressure P_{TM} (left panel) and stapes velocity V_S (center panel) at the frequencies f_1 , f_2 , and $f_{dp}=2f_1-f_2$. The right-hand panel shows the corresponding forward and reverse middle-ear transfer functions, \vec{T}_S and \overleftarrow{T}_S . Note that the forward transfer functions computed from measurements at f_1 and f_2 superimpose. Measurements are from cat 58.

The five forward transfer functions $\vec{T}_S(f)$ share some features (Fig. 5, left). Transmission magnitudes increase with frequency at low frequencies, reach a maximum between 1 and 2 kHz, and generally decrease at higher frequencies. Additionally, all angles decrease as frequency increases. The data are similar to corresponding measurements of Guinan and Peake (1967), which were made using stroboscopic illumination, and to the model of Puria and Allen (1998).

The five reverse transfer functions $\overleftarrow{T}_S(f)$ also share some features (Fig. 5, right). Reverse transmission has a magnitude minimum between 1 and 3 kHz, followed by a

local magnitude maximum within an octave of the minimum. The angles have a local maximum that corresponds with the rapid increase in the magnitude that occurs between the magnitude minimum and maximum. Similar features are also predicted by the model of Puria and Allen (1998) when the ear canal is terminated by Z_{SRC} (Sec. II J).

C. Impedance measurements

Figure 6 shows that the impedances at the eardrum $Z_{TM}(f)$ on all five ears share many features. These include a

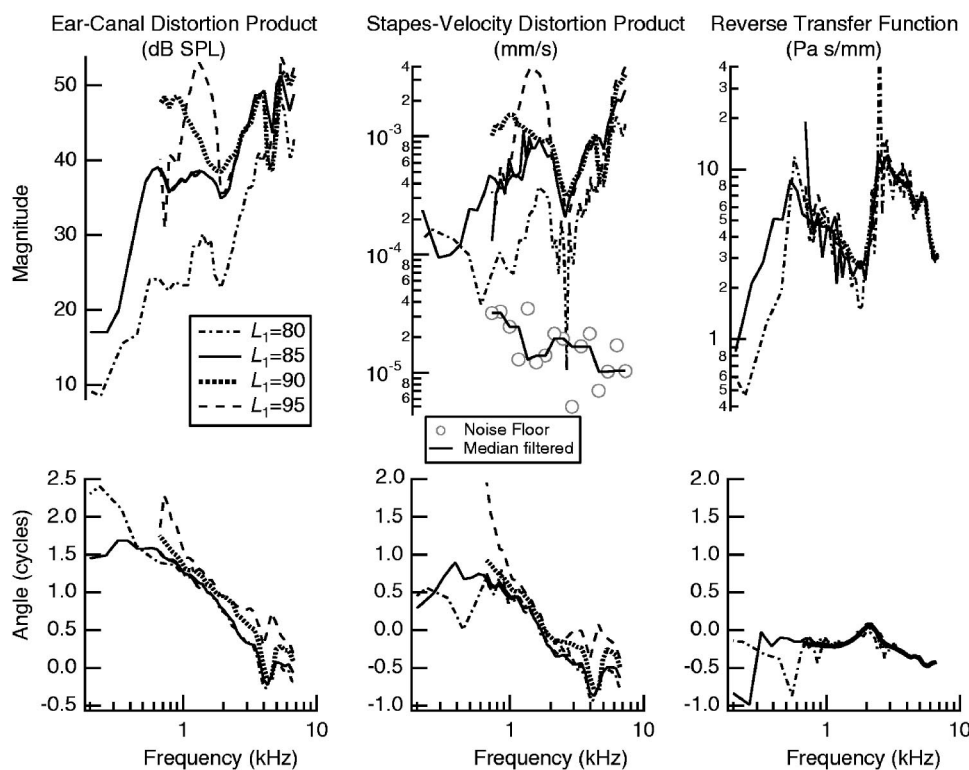


FIG. 4. Left: Measurements of the $2f_1-f_2$ component of the eardrum pressure, $P_{TM}(f_{dp})$. In all cases, $L_2 = L_1 - 5$ dB. Center: The distortion-product component of the stapes velocity, $V_S(f_{dp})$. Right: The reverse transfer function, $\overleftarrow{T}_S(f)$. The data points marked “noise floor” on the magnitude plot of the stapes velocity result from a velocity measurement made with no stimulus. Primary levels are indicated by L_1 and L_2 , corresponding to the tones at f_1 and f_2 , respectively. All measurements are from cat 58, which was the only preparation stable enough to permit a series of measurements at several stimulus levels.

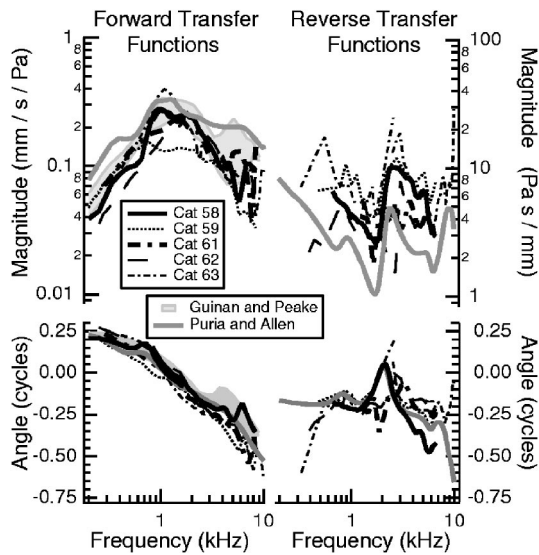


FIG. 5. Magnitudes (upper) and angles (lower) of the simultaneous measurements of $\bar{T}_S(f)$ (left) and $\bar{T}_S(f)$ (right) in five ears. The gray shaded region indicates the range of the forward transfer function measured by Guinan and Peake (1967) on 4 ears. Transfer functions computed using the model of Puria and Allen (1998) are shown for comparison.

stiffness-dominated behavior below 1 kHz (i.e., an impedance magnitude that decreases at about 6 dB per octave and an angle of roughly -0.25 cycles) and a mixed impedance at higher frequencies. Our impedance measurements are similar to those of Puria and Allen (1998) and Lynch *et al.* (1994), except that on average our low-frequency magnitudes are a few dB lower than the Lynch *et al.* (1994) measurements. These differences may reflect the relatively small animals

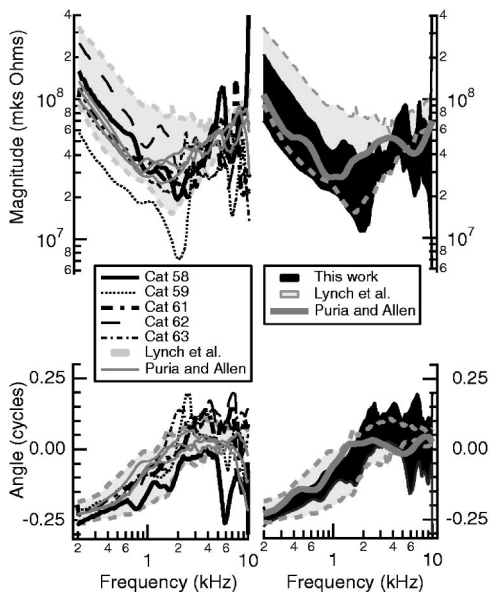


FIG. 6. Magnitudes (upper) and angles (lower) of the middle-ear impedance, $Z_{TM}(f)$. Left: The impedances measured on the five ears discussed here. Shown for comparison are those reported by Lynch *et al.* (1994) (lightly shaded region enclosed by the dashed lines) and Puria and Allen (1998) (three individuals in gray). Right: The mean and standard deviation for the impedances measured here (dark shaded region). Magnitude means and standard deviations were computed on a log scale. The solid gray line shows Z_{TM} computed using the Puria and Allen (1998) model. The range of values measured by Lynch *et al.* (1994) is enclosed by the dashed gray lines.

employed in our study: According to Lynch *et al.* (1994, Fig. 17), low-frequency impedance magnitudes decrease with body mass. The Puria and Allen (1998) model and measurements are closer to our measurements: Both their model and data have low-frequency magnitudes that are similar to ours and both have angles that are not mass dominated but instead noodle about zero.

IV. DISCUSSION

A. Towards a two-port description of the middle ear

The linearity of middle-ear mechanics below the acoustic-reflex threshold (e.g., Guinan and Peake, 1967; Nedzelnitsky, 1980; Cooper and Rhode, 1992) implies that the middle ear can be completely characterized in terms of its response to pure tones. Since the cochlear contents appear essentially incompressible at audio frequencies (Voss *et al.*, 1996; Shera and Zweig, 1992a), the complex pressures and volume velocities on either side of the middle ear are related by a “transfer matrix,” $\mathbf{T}_{ME}(f)$ (Shera and Zweig, 1992b). The 2×2 matrix $\mathbf{T}_{ME}(f)$ relates the input and output of the middle ear. The two input variables are the pressure at the tympanic membrane (P_{TM}) and the volume velocity at the tympanic membrane (U_{TM}), and the two output variables are the pressure across the cochlear partition (P_C) and the volume velocity of the stapes (U_S). The matrix $\mathbf{T}_{ME}(f)$ is defined by the equation

$$\begin{pmatrix} P_{TM} \\ U_{TM} \end{pmatrix} = \mathbf{T}_{ME} \begin{pmatrix} P_C \\ U_S \end{pmatrix}, \quad (4)$$

with the four complex matrix elements of $\mathbf{T}_{ME}(f)$ denoted by $\begin{pmatrix} A & B \\ C & D \end{pmatrix}$. The matrix elements of $\mathbf{T}_{ME}(f)$ have simple interpretations obtained by considering specific loading conditions (Shera and Zweig, 1992b). If the stapes is immobilized so that $U_S = 0$, then $A = P_{TM}/P_C$ and $C = U_{TM}/P_C$. In other words, A^{-1} is the “infinite-load” forward pressure transfer ratio and C^{-1} is the “infinite-load” forward transfer impedance. If $P_C = 0$ (e.g., if the cochlear fluids are drained), then $B = P_{TM}/U_S$ and $D = U_{TM}/U_S$. In other words, B^{-1} is the “no-load” forward transfer admittance and D^{-1} is the “no-load” forward velocity transfer ratio.

The matrix $\mathbf{T}_{ME}(f)$ provides a meaningful description of the middle ear whenever the four variables defining the transformation constitute the effective input and output of the system. So long as the input and output are effectively one-dimensional, the vibration of the eardrum and ossicles can be arbitrarily complicated, involving complex motions in all three spatial dimensions (e.g., Decraemer *et al.*, 1991). On the input side, the pressure in the cat ear canal a few millimeters from the eardrum is approximately uniform in any cross section at frequencies less than roughly 20 kHz (Lynch, 1981; Rosowski *et al.*, 1988). On the output side, measurements near the oval window in the basal turn are consistent with the “long-wavelength approximation,” indicating that the pressure is essentially uniform across the stapes footplate, at least for frequencies much less than the local characteristic frequency (Nedzelnitsky, 1980). In addition, the motion of the stapes is largely one-dimensional (“piston-like”) in cat (Guinan and Peake, 1967; Decraemer, 2004b),

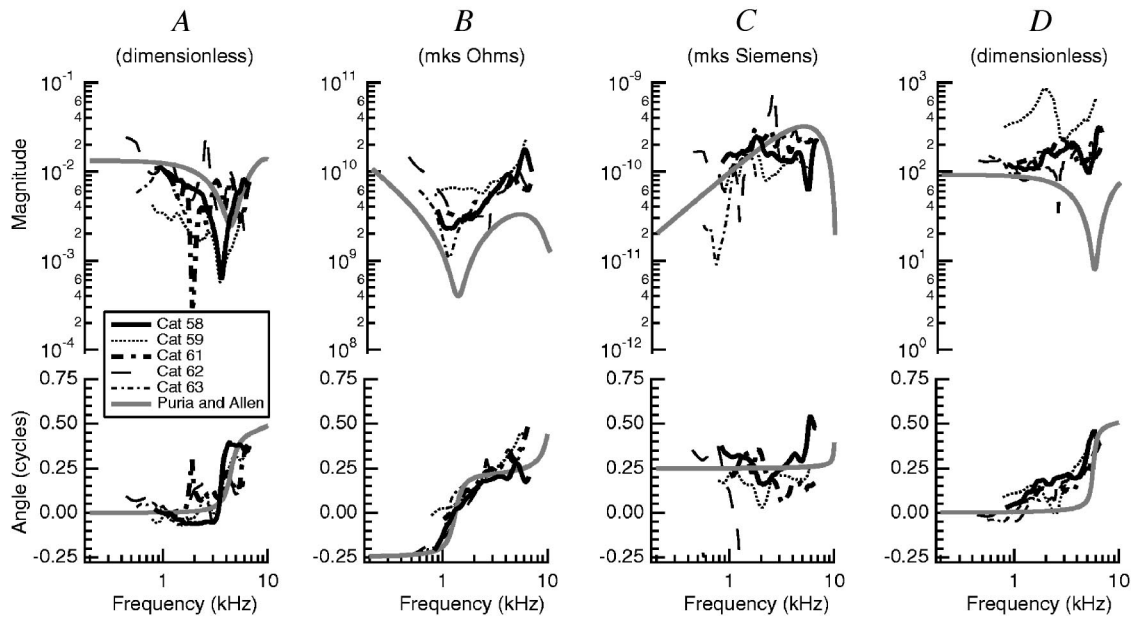


FIG. 7. Magnitudes (upper) and angles (lower) of the matrix elements A , B , C , and D computed [Eq. (A4)] using our data and Lynch *et al.*'s (1982) model of Z_C . Matrix elements computed from the Puria and Allen (1998) model are shown for comparison.

allowing us to estimate stapes volume velocity as the product of measured stapes velocity and the area of the footplate.

Although the matrix $\mathbf{T}_{ME}(f)$ characterizes the transmission properties of the middle ear in a manner independent of any sources or loads presented to it, experimental determination of the elements of $\mathbf{T}_{ME}(f)$ requires knowledge and/or manipulation of the loads at both ends of the middle-ear system. The two loads in our preparation are (1) the combination of the Thévenin impedance of the transducer inserted in the ear canal and the air space between the transducer and the tympanic membrane, Z_{SRC} , and (2) the cochlear input impedance, Z_C . Although Z_{SRC} is known (Sec. II J), Z_C cannot be measured directly without inserting pressure transducers into the cochlear vestibule, a procedure that can introduce bubbles or other artifacts that modify the effective value of Z_C one seeks to measure. Fortunately, the value of Z_C can be determined without direct measurement if its value can be manipulated in some way (e.g., if the impedance can be reduced effectively to zero by draining the cochlear fluids). At every frequency five independent, complex measurements are then needed to determine the four matrix elements of \mathbf{T}_{ME} and the value of Z_C (five equations determine five unknowns). At least one of these measurements must be obtained while driving the middle ear “in reverse” (i.e., from within the inner ear). Perhaps the five most convenient measurements are (1) the middle-ear input impedance; (2) the forward and (3) reverse stapes-velocity transfer functions; (4) the “no-load” (or “short-circuit”) middle-ear input impedance; and (5) the “no-load” forward stapes transfer function. The “no-load” conditions refer to measurements made with the cochlear fluids drained (e.g., Allen, 1986).

B. Estimates of the matrix elements

The measurements presented here (i.e., forward and reverse transmission and ear-canal impedance) provide only three of the five measurements² necessary to determine \mathbf{T}_{ME}

and Z_C . Nevertheless, we can use our measurements to estimate all four matrix elements of \mathbf{T}_{ME} by (1) applying the principle of reciprocity to obtain the additional constraint $\det \mathbf{T}_{ME} = 1$ (e.g., Shera and Zweig, 1991) and (2) using values of Z_C measured in other preparations (e.g., Lynch *et al.*, 1982). Assuming that the middle ear is indeed a reciprocal mechanical system, this procedure should yield accurate estimates of \mathbf{T}_{ME} at frequencies where the matrix elements are not especially sensitive to the value of Z_C . Expressions for the four matrix elements $\begin{pmatrix} A & B \\ C & D \end{pmatrix}$ in terms of Z_{TM} , \vec{T}_S , \overleftarrow{T}_S , Z_{SRC} , and Z_C can be found in the Appendix.

Figure 7 shows our estimates of the matrix elements of $\mathbf{T}_{ME}(f)$ obtained in this way. For simplicity, we approximate Lynch *et al.*'s (1982) measurements of Z_C by their circuit model, which provides a good description of their averaged data. The Appendix demonstrates that the estimates of A and C [Eq. (A4)] do not depend on the assumed value of Z_C . The measurements and the Puria and Allen (1998) model show similar patterns for both the magnitude and angle of A at most frequencies. The model and measurements of C are similar in their order of magnitude and overall form, but there are no clear similarities in the finer details.

The estimates for B and D [Eq. (A4)] assume the Lynch *et al.* (1982) form for the cochlear impedance Z_C . To assess the sensitivity of our estimates of B and D to the assumed value of Z_C , we calculated B and D for all preparations and from the model³ (Puria and Allen, 1998) using a range of values for Z_C . Lynch *et al.* (1982) demonstrate interanimal variations in measured impedance magnitude that span a range of roughly 20 dB (from about $|Z_C|/3$ to $3|Z_C|$). The effects on B and D of similar variations in $|Z_C|$ are shown for cat 58 and for the model by the shaded regions in Fig. 8. (We did not vary the phase of Z_C ; Lynch *et al.*'s model Z_C is essentially resistive over the frequency region explored here.) The effects in other preparations were similar to those in cat 58. At most frequencies the parameters B and D de-

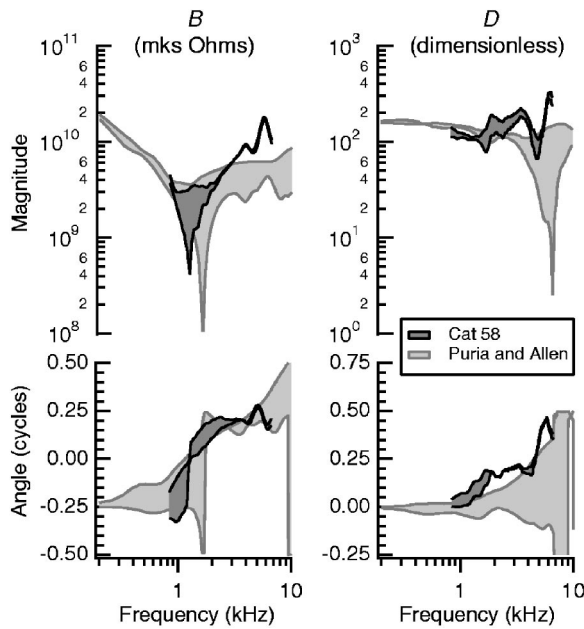


FIG. 8. Sensitivity of the calculations for the matrix elements B (left) and D (right) to the value of the cochlear impedance magnitude $|Z_C|$. The shaded regions enclose the maximum and minimum of the range of magnitude (top) and angle (bottom) values for B and D calculated when $|Z_C|$ was varied up and down by a factor of 3 about its base magnitude. Variations are plotted from measurements on cat 58 (shaded dark gray between black lines) and from the Puria and Allen (1998) model (shaded between gray lines).

rived from the measurements appear more sensitive to individual variations among ears (Fig. 7) than to the imposed variations in $|Z_C|$ (Fig. 8). Thus, at most frequencies, our estimates of B and D appear not to depend substantially on our choice of Z_C . The measurement-based estimates for B are generally similar to the results from the model, while the measurement-based estimates for D differ systematically from the model in both magnitude and angle. The model-based parameters appear more sensitive than the measurement-based parameters to imposed variations in $|Z_C|$.⁴

C. Reverse transmission and the ear-canal load impedance

Just as forward middle-ear transmission depends on the cochlear input impedance, reverse transmission depends on the impedance that loads the ear canal (e.g., Matthews, 1983; Rosowski *et al.*, 1984; Zwicker, 1990; Puria and Rosowski, 1996; Puria, 2003). The two-port description of the middle ear makes this dependence explicit:

$$\overleftarrow{T}_S = \frac{A_S Z_{REV}}{A + C Z_{REV}}, \quad (5)$$

where Z_{REV} is the reverse impedance at the tympanic membrane directed into the ear canal towards the outer ear, and A_S is the area of the stapes footplate. [Equation (5) is derived in the Appendix as Eq. (A3).] Equation (5) implies that \overleftarrow{T}_S is approximately independent of the reverse ear-canal impedance Z_{REV} only if $|Z_{TM}^\infty| \ll |Z_{REV}|$, where $Z_{TM}^\infty \equiv A/C$. (Note that $|A/C|$ is the value of Z_{TM} when the cochlear load is infinite; e.g., when the stapes is fixed.) Figure 9 shows that

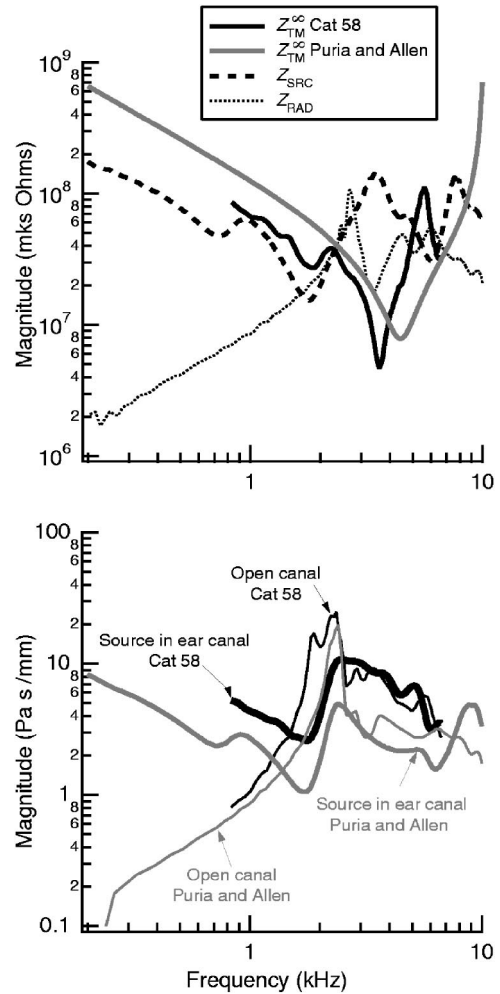


FIG. 9. Upper: Magnitudes of relevant impedances that determine the reverse-transfer function with both the source in the ear canal and the ear canal open to the environment. Z_{SRC} is the Thévenin source equivalent of the earphone and the ear-canal air space; Z_{RAD} is the radiation impedance from the cat ear canal measured by Rosowski *et al.* (1988); and Z_{TM}^∞ is the ratio A/C calculated from the measurements and the model. Lower: Magnitude of the reverse transfer function as measured with the source in the ear canal, and as predicted for the ear canal open to the environment from both cat 58 data and the model.

this condition is almost never satisfied for representative values of Z_{REV} . The upper panel plots $|Z_{TM}^\infty|$ estimated from the data and also from the Puria and Allen (1998) model. Also plotted are two different values of the reverse ear-canal load impedance Z_{REV} : (1) the ear-canal air space and the Thévenin source impedance of the acoustic transducer used here (Z_{SRC}) and (2) the radiation impedance of a cat's ear measured at the tympanic membrane (Z_{RAD}) (Rosowski *et al.*, 1988). With the exception of a narrow frequency interval near 3.5 kHz, $|Z_{TM}^\infty|$ is always comparable to or greater than $|Z_{REV}|$. Indeed, when the ear canal is open to the environment the opposite limit (i.e., $|Z_{TM}^\infty| \gg |Z_{REV}|$) pertains at frequencies less than about 1.5 kHz. Consequently, the reverse transfer function is always strongly dependent on the ear-canal load. We illustrate this dependence in the lower panel of Fig. 9, which plots $|\overleftarrow{T}_S|$ for both terminating impedances. The transfer-function magnitudes are similar in the two cases at frequencies above 2 kHz (where $|Z_{SRC}|$ and $|Z_{RAD}|$ are

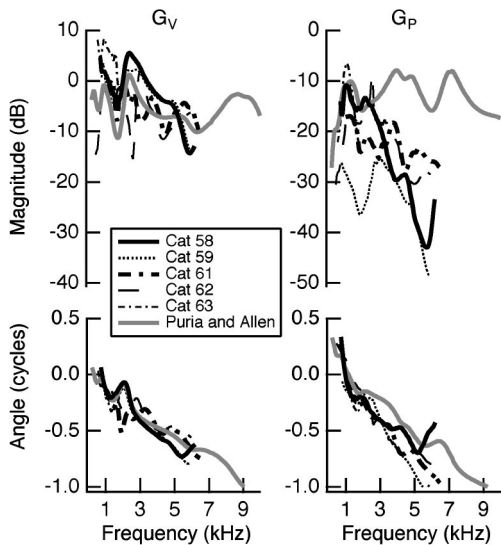


FIG. 10. Left: Magnitude (upper) and angle (lower) of G_V , the round-trip middle-ear velocity gain. A linear fit to all angle data (1 to 5.5 kHz) has a slope corresponding to a delay of 110 μs . Right: Magnitude (top) and angle (bottom) of G_P , the round-trip middle-ear pressure gain. A linear fit to all angle data (1 to 5.5 kHz) has a slope corresponding to a delay of 162 μs .

similar) but differ substantially at lower frequencies (where $|Z_{\text{SRC}}|$ and $|Z_{\text{RAD}}|$ diverge from one another).

D. Round-trip middle-ear gain

The product of the forward and reverse middle-ear pressure transfer functions provides a measure of the total middle-ear gain for otoacoustic emissions reemitted at the stimulus frequency (e.g., SFOAEs and TEOAEs). In these cases, a signal in the ear canal travels through the middle ear (with a gain and phase shift described by the forward transfer function), is reemitted by the cochlea, and travels in reverse through the middle ear back to the ear canal (described by the reverse transfer function). Thus, the product of the forward and reverse middle-ear pressure transfer functions describes the middle ear's influence on these emissions measured in the ear canal. Puria (2003) names this product the "round-trip pressure gain."

Here we define G_V as the product of forward and reverse stapes velocity transfer functions:

$$G_V = \vec{T}_S(f) \tilde{T}_S(f). \quad (6)$$

The round-trip pressure gain, G_P , can be written in terms of G_V as⁵

$$G_P = \left(\frac{P_C}{P_{\text{EC}}}\bigg|_{\text{forward}} \right) \left(\frac{P_{\text{EC}}}{P_C}\bigg|_{\text{reverse}} \right) = \frac{\vec{Z}_C}{\tilde{Z}_{\text{ME}}} G_V, \quad (7)$$

where \vec{Z}_C is the input impedance of the cochlea (here written with an arrow to emphasize that the system is driven in the forward direction) and $\tilde{Z}_{\text{ME}} = P_C/U_S$ is the reverse middle-ear (or cochlear output) impedance measured looking out from the cochlea toward the ear canal.

Figure 10 plots G_V and G_P for our five preparations along with those calculated from the model. The magnitude of the velocity gain $|G_V|$ waxes and wanes between -15 and 5 dB, and the magnitude of the pressure gain $|G_P|$ is about

20 dB below that of the velocity gain $|G_V|$. The mean group delays of G_V and G_P provide two different measures of the round-trip delay through the middle ear. Fitting a straight line to the phase data (from 1 to 5.5 kHz) yields mean round-trip delays of 110 ± 4 and 162 ± 6 μs , respectively, where the uncertainties are approximate 95% confidence intervals. In each case, the linear fits account for approximately 80% of the total variance of the data. The mean round-trip group delays found here are similar to those predicted by the Puria and Allen (1998) model of 125 ± 4 and 145 ± 6 μs for G_V and G_P , respectively (again computed from 1 to 5.5 kHz).⁶

V. SUMMARY

We have demonstrated a technique for measuring middle-ear impedance and forward/reverse middle-ear transmission in the same cat ear (with widely opened middle-ear cavities). The method uses DPOAEs as an intracochlear sound source to drive the middle ear "in reverse" without opening the inner ear. The measured forward transfer functions and input impedances generally agree with previous measurements, and the measured forward and reverse transfer functions and the input impedances agree qualitatively with model predictions. In addition, we have developed a measurement-based framework for determining the equivalent two-port network (i.e., transfer or $ABCD$ matrix) that characterizes the transmission properties of the cat middle ear. Using this framework we have estimated the matrix elements by combining the measurements presented here with published measurements of the cochlear input impedance.

ACKNOWLEDGMENTS

This work was supported by Grant No. R01 DC03687 from the NIDCD. We gratefully acknowledge the help of Leslie Liberman, who assisted with animal care and preparation, and thank Willem F. Decraemer, John J. Rosowski, and William T. Peake for useful discussions. We thank Sunil Puria for sharing his computer code to compute the responses of his model. William T. Peake, Douglas H. Keefe, and an anonymous reviewer provided helpful comments on the manuscript.

APPENDIX: SOLVING FOR THE MATRIX ELEMENTS OF \mathbf{T}_{ME}

In this Appendix we derive equations that express the four matrix elements of \mathbf{T}_{ME} in terms of the middle-ear input impedance (Z_{TM}) and the forward and reverse stapes-velocity transfer functions (\vec{T}_S and \tilde{T}_S). We assume that the middle ear is a reciprocal mechanical system ($\det \mathbf{T}_{\text{ME}} = 1$) and that both the Thévenin-equivalent impedance of the measurement transducer, including the residual ear-canal space (Z_{SRC}), and the cochlear input impedance (Z_C) are known.

We begin by expressing the three measured quantities in terms of the matrix elements of $\mathbf{T}_{\text{ME}} \equiv \begin{pmatrix} A & B \\ C & D \end{pmatrix}$ defined by Eq. (4):

$$Z_{\text{TM}} = \frac{AZ_C + B}{CZ_C + D}; \quad (A1)$$

$$\vec{T}_S = \frac{1}{A_S} \frac{1}{AZ_C + B}; \quad (\text{A2})$$

and

$$\overleftarrow{T}_S = \frac{A_S}{A/Z_{\text{SRC}} + C}. \quad (\text{A3})$$

Note that the area of the stapes footplate, $A_S = 1.15 \times 10^{-2} \text{ cm}^2$ as reported by Wever and Lawrence (1954), has been used to convert stapes volume velocity (used in the definitions of \mathbf{T}_{ME} and Z_C) to stapes velocity (used in the definitions of \vec{T}_S and \overleftarrow{T}_S). When the middle ear is driven in reverse we adopt the convention that positive volume velocity flows into the middle ear at the stapes and out at the eardrum. [The signs of U_S and U_{EC} are therefore reversed relative to the convention adopted in Eq. (4); when the middle ear is driven in the forward direction, positive volume velocity flows into the middle ear at the ear drum and out at the stapes.]

When combined with the constraint of reciprocity (which requires $\det \mathbf{T}_{\text{ME}} = 1$), Eqs. (A1)–(A3) provide four equations that can be solved for the four matrix elements $\begin{pmatrix} A & B \\ C & D \end{pmatrix}$. The solution is

$$\mathbf{T}_{\text{ME}}(f) = \begin{pmatrix} P/Q & 1/\vec{T}_S A_S - Z_C P/Q \\ R/Q & (1 - \vec{T}_S A_S Z_C Z_{\text{TM}} R/Q) / \vec{T}_S A_S Z_{\text{TM}} \end{pmatrix}, \quad (\text{A4})$$

where

$$Q \equiv \frac{\overleftarrow{T}_S}{A_S} (Z_{\text{SRC}} + Z_{\text{TM}}); \quad (\text{A5})$$

$$P \equiv Z_{\text{TM}} Z_{\text{SRC}} (1 + \vec{T}_S \overleftarrow{T}_S); \quad (\text{A6})$$

and

$$R \equiv Z_{\text{SRC}} - \vec{T}_S \overleftarrow{T}_S Z_{\text{TM}}. \quad (\text{A7})$$

¹The optimized lengths of the six closed brass cylindrical tubes used to determine the Thévenin equivalent were 17.64, 23.45, 28.21, 37.52, 46.48, and 64.08 mm, and the lengths of the five additional tubes used to check the Thévenin equivalent were 20.25, 26.37, 33.97, 40.47, and 53.64 mm. The lengths on these five additional tubes were determined using the same procedures used to determine Z_{Th} . The radii of all tubes were $r = 2.8 \text{ mm}$.

²We made no measurements in the drained-cochlea condition because by the end of each experiment reported here substantial blood clots had formed around the incudo-stapedial joint. Future attempts at measurements with a drained cochlea should be made within a few hours of the start of the experiment, rather than 12–24 h after the start.

³The model of Puria and Allen (1998) uses the theoretical Z_C estimated by Puria and Allen (1991) rather than the measurements of Lynch *et al.* (1982).

⁴When the Lynch *et al.* (1982) measurement-based Z_C is used with the Puria and Allen (1998) model, variations in B and D are somewhat smaller than with the model-based Z_C from Puria and Allen (1991).

⁵Puria (2003) defines the round-trip pressure gain in terms of the pressure P_V measured in the vestibule rather than the pressure P_C measured across the cochlear partition. Since the pressure in the vestibule is much larger than the pressure in the scala tympani (Nedzelniisky, 1980), the difference between these two pressures is minor.

⁶In gerbil Olson (1998) reports a forward delay of about $25 \mu\text{s}$.

- Allen, J. B. (1986). "Measurement of eardrum acoustic impedance," in *Peripheral Auditory Mechanisms*, edited by J. B. Allen, J. L. Hall, A. Hubbard, S. T. Neely, and A. Tubis (Springer-Verlag, New York), pp. 44–51.
- Avan, P., Büki, B., Maat, B., Dordain, M., and Wit, H. P. (2000). "Middle ear influence on otoacoustic emissions. I: Noninvasive investigation of the human transmission apparatus and comparison with model results," *Hear. Res.* **140**, 189–201.
- Buunen, T. J. F., and Vlaming, M. (1981). "Laser-Doppler velocity meter applied to tympanic membrane vibrations in cat," *J. Acoust. Soc. Am.* **69**, 744–750.
- Cooper, N. P., and Rhode, W. S. (1992). "Basilar membrane mechanics in the hook region of cat and guinea-pig cochlea: Sharp tuning and nonlinearity in the absence of baseline position shifts," *Hear. Res.* **63**, 163–190.
- Decraemer, W. F. (2004a). Personal communication.
- Decraemer, W. F. (2004b). *Measurement, Visualization and Quantitative Analysis of Complete Three-dimensional Kinematical Data Sets of Human and Cat Middle Ear* (World Scientific, Singapore, in press).
- Decraemer, W. F., Khanna, S. M., and Funnell, W. R. J. (1991). "Malleus vibration model changes with frequency," *Hear. Res.* **54**, 305–318.
- Guinan, J. J., and Peake, W. T. (1967). "Middle-ear characteristics of anesthetized cats," *J. Acoust. Soc. Am.* **41**, 1237–1261.
- Huang, G. T., Rosowski, J. J., Flandermeyer, D. T., Lynch, T. J., and Peake, W. T. (1997). "The middle ear of a lion: Comparison of structure and function to domestic cat," *J. Acoust. Soc. Am.* **101**, 1532–1549.
- Huang, G. T., Rosowski, J. J., Puria, S., and Peake, W. T. (2000a). "A noninvasive method for estimating acoustic admittance at the tympanic membrane," *J. Acoust. Soc. Am.* **108**, 1128–1146.
- Huang, G. T., Rosowski, J. J., Puria, S., and Peake, W. T. (2000b). "Tests of some common assumptions of ear-canal acoustics in cats," *J. Acoust. Soc. Am.* **108**, 1147–1161.
- Keefe, D. H., Ling, R., and Bulen, J. C. (1992). "Method to measure acoustic impedance and reflection coefficient," *J. Acoust. Soc. Am.* **91**, 470–485.
- Lynch, T. J. (1981). "Signal processing by the cat middle ear: Admittance and transmission, measurements and models," Ph.D. thesis, Massachusetts Institute of Technology.
- Lynch, T. J., Nedzelniisky, V., and Peake, W. T. (1982). "Input impedance of the cochlea in cat," *J. Acoust. Soc. Am.* **72**, 108–130.
- Lynch, T. J., Peake, W. T., and Rosowski, J. J. (1994). "Measurements of the acoustic input impedance of cat ears: 10 Hz to 20 kHz," *J. Acoust. Soc. Am.* **96**, 2184–2209.
- Magnan, P., Avan, P., Dancer, A., Smurzynski, J., and Probst, R. (1997). "Reverse middle-ear transfer function in the guinea pig measured with cubic difference tones," *Hear. Res.* **107**, 41–45.
- Magnan, P., Dancer, A., Probst, R., Smurzynski, J., and Avan, P. (1999). "Intracochlear acoustic pressure measurements: Transfer functions of the middle ear and cochlear mechanics," *Audiol. Neuro-Otol.* **4**, 123–128.
- Matthews, J. W. (1983). "Modeling reverse middle-ear transmission of acoustic distortion products," in *Mechanics of Hearing*, edited by E. de Boer and M. A. Viergever (Martinus Nijhoff, The Hague), pp. 11–18.
- Merchant, S. N., and Rosowski, J. J. (2003). "Auditory physiology," in *Surgery of the Ear* (Decker, Hamilton, Ontario), pp. 59–82.
- Møller, A. R. (1965). "An experimental study of the acoustic impedance of the middle ear and its transmission properties," *Acta Oto-Laryngol.* **60**, 129–149.
- Nedzelniisky, V. (1980). "Sound pressures in the basal turn of the cat cochlea," *J. Acoust. Soc. Am.* **68**, 1676–1689.
- Neely, S. T., and Gorga, M. P. (1998). "Comparison between intensity and pressure as measures of sound level in the ear canal," *J. Acoust. Soc. Am.* **104**, 2925–2934.
- Olson, E. S. (1998). "Observing middle and inner ear mechanics with novel intracochlear pressure sensors," *J. Acoust. Soc. Am.* **103**, 3445–3463.
- Puria, S. (2003). "Measurements of human middle ear forward and reverse acoustics: Implications for otoacoustic emissions," *J. Acoust. Soc. Am.* **113**, 2773–2789.
- Puria, S. (2004). "Middle-ear two-port measurements in human cadaveric temporal bones: Comparison with models," in *Middle Ear Mechanics in Research and Otology*, edited by A. Gyo and H. Wada (World Scientific, Singapore).
- Puria, S., and Allen, J. (1998). "Measurements and model of the cat middle ear: Evidence of tympanic membrane acoustic delay," *J. Acoust. Soc. Am.* **104**, 3463–3481.

- Puria, S., and Allen, J. B. (1991). "A parametric study of cochlear input impedance," *J. Acoust. Soc. Am.* **89**, 287–309.
- Puria, S., and Rosowski, J. J. (1996). "Measurement of reverse transmission in the human middle ear: Preliminary results," in *Proceedings of the International Symposium on Diversity in Auditory Mechanics*, edited by E. R. Lewis, G. R. Long, R. Lyon, P. Narins, C. Steele, and E. Hecht-Poinar (World Scientific, Singapore), pp. 151–157.
- Puria, S., Peake, W. T., and Rosowski, J. J. (1997). "Sound-pressure measurements in the cochlear vestibule of human-cadaver ears," *J. Acoust. Soc. Am.* **101**, 2754–2770.
- Rabinowitz, W. M. (1981). "Measurement of the acoustic input immittance of the human ear," *J. Acoust. Soc. Am.* **70**, 1025–1035.
- Rosowski, J. J., Peake, W. T., and White, J. (1984). "Cochlear nonlinearities inferred from two-tone distortion products in the ear canal of the alligator lizard," *Hear. Res.* **13**, 141–158.
- Rosowski, J. J., Carney, L. H., and Peake, W. T. (1988). "The radiation impedance of the external ear of cat: Measurements and applications," *J. Acoust. Soc. Am.* **84**, 1695–1708.
- Shera, C. A., and Guinan, J. J. (1999). "Evoked otoacoustic emissions arise by two fundamentally different mechanisms: A taxonomy for mammalian OAEs," *J. Acoust. Soc. Am.* **105**, 782–798.
- Shera, C. A., and Zweig, G. (1991). "Phenomenological characterization of eardrum transduction," *J. Acoust. Soc. Am.* **90**, 253–262.
- Shera, C. A., and Zweig, G. (1992a). "An empirical bound on the compressibility of the cochlea," *J. Acoust. Soc. Am.* **92**, 1382–1388.
- Shera, C. A., and Zweig, G. (1992b). "Middle-ear phenomenology: The view from the three windows," *J. Acoust. Soc. Am.* **92**, 1356–1370.
- Tonndorf, J., and Tabor, J. R. (1962). "Closure of the cochlear windows: Its effect upon air- and bone-conduction," *Ann. Otol. Rhinol. Laryngol.* **71**, 5–29.
- Voss, S. E. (1998). "Effects of tympanic-membrane perforations on middle-ear sound transmission: measurements, mechanisms, and models," Ph.D. thesis, Massachusetts Institute of Technology.
- Voss, S. E., and Allen, J. B. (1994). "Measurement of acoustic impedance and reflectance in the human ear canal," *J. Acoust. Soc. Am.* **95**, 372–384.
- Voss, S. E., and Shera, C. (2002). "Simultaneous measurement of DPOAEs, middle-ear input impedance, and forward/reverse middle-ear transmission in cat," *Assoc. Res. Otolaryngol. Abs.* **25**, 585.
- Voss, S. E., Rosowski, J. J., and Peake, W. T. (1996). "Is the pressure difference between the oval and round windows the effective acoustic stimulus for the cochlea?" *J. Acoust. Soc. Am.* **100**, 1602–1616.
- Voss, S. E., Rosowski, J. J., Merchant, S. N., and Peake, W. T. (2000). "Acoustic responses of the human middle ear," *Hear. Res.* **150**, 43–69.
- Wever, E. G., and Lawrence, M. (1954). *Physiological Acoustics* (Princeton U.P., Princeton).
- Zwicker, E. (1990). "On the influence of acoustical probe impedance on evoked otoacoustic emissions," *Hear. Res.* **47**, 185–190.